# Two convergent triangle tunnels

Boris Odehnal

November 13, 2018

## Abstract

A semi-orthogonal path is a polygon inscribed into a given polygon such that the $i$-th side of the path is orthogonal to the $i$-th side of the given polygon. Especially in the case of triangles, the closed semi-orthogonal paths are triangles which turn out to be similar to the given triangle. The iteration of the construction of semi-orthogonal paths in triangles yields infinite sequences of nested and similar triangles. We show that these two different sequences converge towards the bicentric pair of the triangle's Brocard points. Furthermore, the relation to discrete logarithmic spirals allows us to give a very simple, elementary, and new constructions of the sequences' limits, the Brocard points. We also add some remarks on semi-orthogonal paths in non-Euclidean geometries and in $n$-gons.

*Keywords:* Triangle, semi-orthogonal path, Brocard points, symmedian point, discrete logarithmic spiral, Tucker-Brocard cubic.

*MSC 2010:* 51A05, 51A20.

# 1 Introduction

## 1.1 Sequences of triangles

Little is known about sequences of Cevian triangles within a given triangle. Sequences of medial triangles and Routh triangles are studied in [3]. There, triangles are considered as triplets of points in the complex plane and a shape function which is actually a complex affine ratio is defined and describes how the shape of a triangle changes during the iteration process. It turns out that the above mentioned classes of triangles converge in shape, in most cases to equilateral triangles.

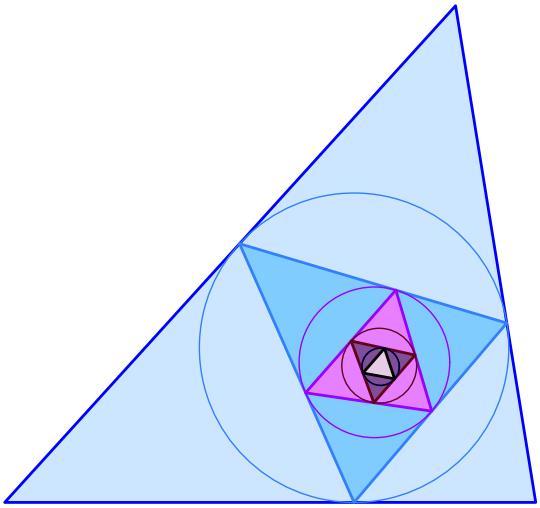

Figure 1: Where and what is the limit of the sequence of intouch triangles?

It is well-known (and rather trivial) that the sequence of Cevian triangles of a triangle's centroid converges towards the centroid. The intouch triangle (contact points of the incircle and the triangle sides) is al-

ways in the interior of the initial triangle (cf. Fig. 1). So, it is nearby to expect that the sequence of nested intouch triangles has a point shaped limit which is yet undiscovered. On the contrary, the orthic triangle is an interior triangle only if the base triangle is acute and, unfortunately, acute triangles may have an obtuse orthic triangle and convergence cannot be expected in the generic case.

We try to leave the beaten tracks by starting the construction of the triangles of the sequence in a different way. The edges of the triangles in the sequences in question shall form a semi-orthogonal path, *i.e.*, the $i$-th edge of the new triangle shall be orthogonal to the $i$-th side of the given triangle. Depending on the ordering of the sides of the base triangle, we find two closed semi-orthogonal paths which shall be constructed and discussed in Sec. 2. Further, the case of generic $n$-laterals ($n$ straight lines in generic position such that no two lines enclose a right angle) shall be addressed in Sec. 2, besides some comments on closed semi-orthogonal paths in non-degenerate Cayley-Klein geometries, *i.e.*, the elliptic and the hyperbolic plane. Sec. 3 is dedicated to the computation of the limits of the triangle sequences. We show that the triangles in one sequence shrink to one Brocard point, while the others converge to the other Brocard point, and thus, these two limits are located on the Tucker-Brocard cubic. Finally, in Sec. 4, we conclude and address some open problems. The remaining part of this section (Sec. 1) collects some prerequisites.

## 1.2 Prerequisites and conventions

Since we deal with triangles in the Euclidean plane $\mathbb{R}^2$, we use Cartesian coordinates in order to describe points. It will turn out useful to perform the projective closure of the Euclidean plane by adding the ideal line $\omega$ to $\mathbb{R}^2$. Whenever, we deal with points and lines in the projectively extended plane, we can switch between Cartesian and homogeneous coordinates of points by

$$(1, x, y) \longleftrightarrow (x_0 : x_1 : x_2)$$

as long as $x_0 \neq 0$. Lines $l: \ a_0 + a_1 x + a_2 x = 0$ can also be described by homogeneous coordinates $(a_0 : a_1 : a_2)$. Especially, the ideal line (or line at infinity) is simply given by $\omega = (1 : 0 : 0)$.

For the moment, it is sufficient to assume that the Cartesian coordinates of the vertices of the base triangle $\Delta_0$ are

$$A_0 = (0, 0), \quad B_0 = (c, 0), \quad C_0 = (u, v). \tag{1}$$

We assume that $c, v \neq 0$ so that $A_0 \neq B_0$ and $C_0 \notin [A_0, B_0]$. Further, $u^2 + v^2 \neq 0$ which implies $A_0 \neq C_0$. In the following, no interior angle of $\Delta_0$ shall be a right one. This is expressed algebraically by $u \neq c$, $u \neq 0$, and $u^2 - uc + v^2 \neq 0$.

We shall agree that the side lengths of $\Delta_0$ are

$$a := \overline{B_0 C_0}, \quad b := \overline{C_0 A_0}, \quad c := \overline{A_0 B_0}.$$

Later, when we try to express especially metric properties of the triangle in terms of $\Delta_0$'s side lengths $a$, $b$, $c$, we should be able to replace $u$ and $v$ from (1) by functions

depending on $a$, $b$, $c$. For that purpose, we compute $C_0 = (u, v)$ as the intersection of two circles: one centered at $A_0$ with radius $b$; the other one centered at $B_0$ with radius $a$ such that $v > 0$. This results in

$$u = \frac{b^2 + c^2 - a^2}{2c} \quad \text{and} \quad v = \frac{2F}{c} \tag{2}$$

with $F$ being the area of $\Delta_0$. Note that $F$ can be expressed in terms of $\Delta_0$'s side lengths using Heron's formula or, equivalently, with help of the Cayley-Menger determinant.

# 2 Closed semi-orthogonal paths

## 2.1 Triangles in the Euclidean plane

Let $\Delta_0 = A_0B_0C_0$ be a triangle in the Euclidean plane. Let further $P_0$ be a point on the side line $[A_0, B_0]$. We construct a sequence $P_0$, $P_1$, $P_2$, $P_3$ of points on the lines $[A_0, B_0]$, $[B_0, C_0]$, $[C_0, A_0]$, $[A_0, B_0]$ in the following way (cf. Fig. 2):

$$P_0 \in [A_0, B_0],\ [P_0, P_1] \perp [A_0, B_0],$$
$$P_1 \in [B_0, C_0]$$
$$\text{with } P_0 \to P_1 \to P_2 \to P_3,$$
$$A_0 \to B_0 \to C_0 \to A_0,$$
$$\text{cyclical replacement.}$$

Henceforth, we shall refer to such paths as *semi-orthogonal paths*. It doesn't make a difference if we start at $[A_0, B_0]$ or at any other side line of $\Delta_0$.

Obviously, the mapping $\pi : P_0 \mapsto P_3$ is a projective mapping $[A_0, B_0] \to [A_0, B_0]$, since it is a chain of three perspectivities:

$$\underbrace{[A_0, B_0] \overset{R^\perp}{\barwedge} [B_0, C_0] \overset{S^\perp}{\barwedge} [C_0, A_0] \overset{T^\perp}{\barwedge} [A_0, B_0]}_{\barwedge}$$

where $R := [A_0, B_0] \cap \omega$, $S := [B_0, C_0] \cap \omega$, and $T := [C_0, A_0] \cap \omega$ are the ideal points of $\Delta_0$'s side lines and $R^\perp$, $S^\perp$, and $T^\perp$ are the ideal points of the respective orthogonal directions. Note, that the three perspectors are collinear as indicated in Fig. 2.

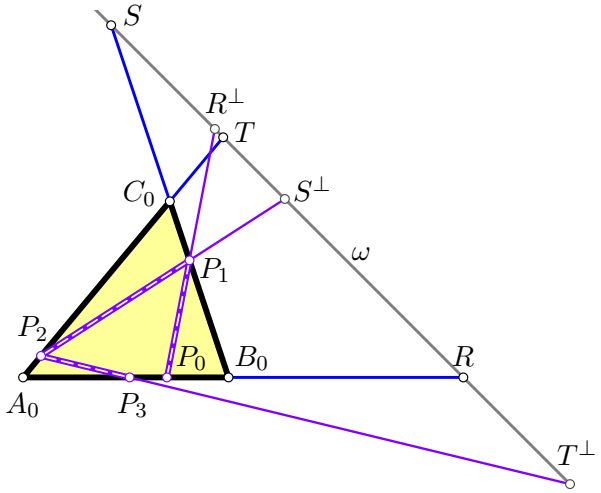


Figure 2: The projective mapping $\pi : [A_0, B_0] \to [A_0, B_0]$ is the product of three perspectivities. The perspectors themselves are assigned to the ideal points of $\Delta_0$'s side lines in a projective way: They are joined by the absolute polarity acting on $\omega$.

**Remark 1.** *Indeed, the projective mapping $\perp : \omega \to \omega$ that assigns the ideal point of the orthogonal direction to any ideal point can be replaced by any other elliptic projective mapping acting on $\omega$. The pseudo-Euclidean case would be covered if $\perp$ is hyperbolic.*

The ideal point $R$ of $[A_0, B_0]$ is self-assigned in $\pi$, since $\pi(R) = R$, and therefore, we can expect only one further fixed point $A_1$ of $\pi$.

Let now, $P_0 = (t, 0)$ with $t \in \mathbb{R}$ which is a parametrization of the line $[A_0, B_0]$ and we find

$$P_1 = \left(t, \tfrac{v(c-t)}{c-u}\right), \quad P_2 = \frac{\alpha(t)}{\beta}(u, v), \quad P_3 = \frac{\alpha(t)(u^2+v^2)}{u\beta}(1, 0) \tag{3}$$

where

$$\begin{aligned} \alpha(t) &= ((c-u)^2+v^2)t - cv^2, \\ \beta &= ((c-u)^2+v^2)u - cv^2. \end{aligned}$$

Note that $c - u$ is a divisor of $\beta$ that cannot vanish due to assumptions made earlier. The path $P_0P_1P_2P_3$ is closed if the points $P_0$ and $P_3$ coincide. This is equivalent to $t = \frac{\alpha(t)}{u\beta}(u^2 + v^2)$, and thus,

$$t = \frac{c(u^2+v^2)}{c^2 - cu + u^2 + v^2}. \tag{4}$$

We shall make explicit the fact that the denominator of $t$ in (4) cannot vanish: Substituting (2) into (4), we find

$$t = 2b^2c\sigma^{-1} \tag{5}$$

where

$$\sigma := a^2 + b^2 + c^2 \tag{6}$$

which cannot vanish for $a, b, c \in \mathbb{R}^\star$.

If we insert (4) into (3) and relabel the points by letting $A_1 = P_0 = P_3$, $B_1 = P_1$, and $C_1 = P_2$, we arrive at

$$A_1 = \tfrac{c}{\gamma}(c(u^2+v^2), 0), \quad B_1 = \tfrac{c}{\gamma}(u^2+v^2, cv), \quad C_1 = \tfrac{cu}{\gamma}(u, v) \tag{7}$$

with $\gamma = c^2 - cu + u^2 + v^2$. Such a closed triangular path $A_1B_1C_1$ is shown in Fig. 3.

As can be seen in Fig. 3,

$$\begin{aligned} \sphericalangle C_1A_1B_1 &= \sphericalangle C_0A_0B_0, \\ \sphericalangle A_1B_1C_1 &= \sphericalangle A_0B_0C_0, \\ \sphericalangle B_1C_1A_1 &= \sphericalangle B_0C_0A_0. \end{aligned}$$

Thus, we have

**Lemma 1.** *The triangles $\Delta_0$ and $\Delta_1$ are similar.*

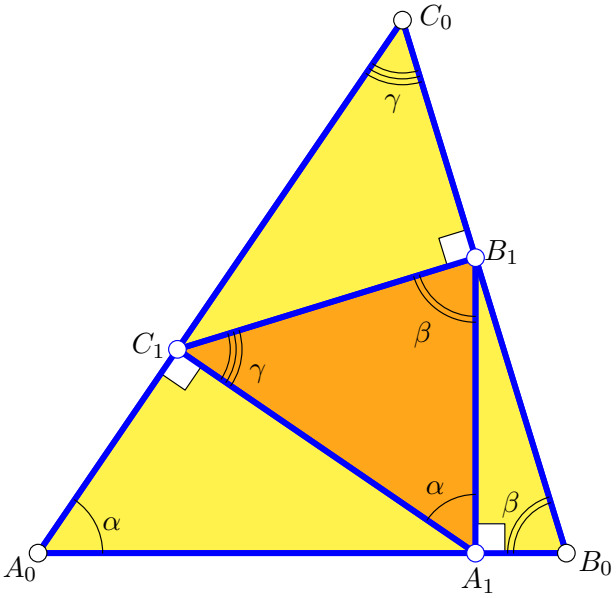


Figure 3: The first triangle $\Delta_1 = A_1B_1C_1$ inscribed into $\Delta_0 = A_0B_0C_0$.

In order to construct the path $A_1B_1C_1$, we started at $P_0$ leaving $[A_0, B_0]$ in the orthogonal direction until we meet $[B_0, C_0]$. We could also look for a path $Q_0Q_1Q_2Q_3$ with $Q_0 = P_0$ and $Q_1 \in [C_0, A_0]$, *i.e.*, leaving $[A_0B_0]$ in the orthogonal direction until we meet $[C_0A_0]$, and so forth. This yields a second closed triangular path if we achieve

$Q_0 = Q_3$. Then, $L_1 = Q_0$, $K_1 = Q_1$, and $M_1 = Q_2$ form a triangle $\nabla_1$, see Fig. 4. Similar to Lem. 1 and due to the same reasoning, we have

**Lemma 2.** *The triangles $\Delta_0$ and $\nabla_1$ are similar.*

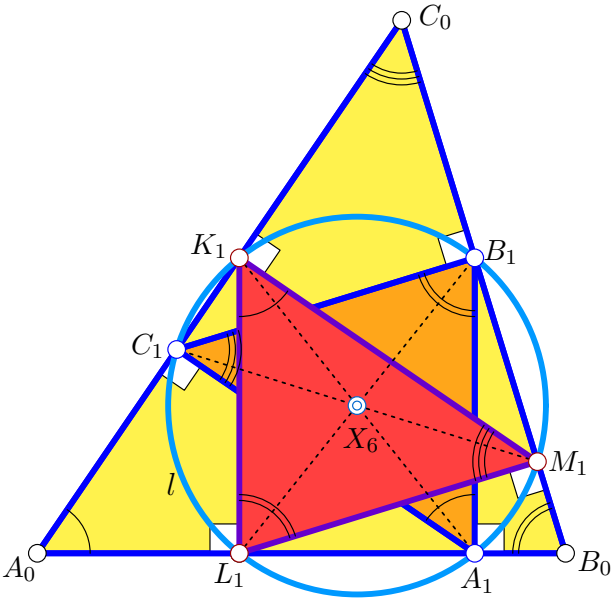


Figure 4: The two perspective triangles $\Delta_1$ and $\nabla_1$ with their common circumcircle (centered at the symmedian point $X_6$).

Moreover, we can show the following

**Theorem 1.** *The triangles $\Delta_1$ and $\nabla_1$ are congruent, share the circumcircle $l$, and therefore, the circumcenter which is the symmedian point $X_6$ of $\Delta_0$.*[1]

*Proof.* The similarity of $\Delta_0$ and $\Delta_1$ needs no further confirmation, since this is done right before Lem. 1. The similarity of $\Delta_0$ and $\nabla_1$ can be shown in the same way. From $\Delta_1 \sim \Delta_0$ and $\nabla_1 \sim \Delta_0$ we can infer $\Delta_1 \sim \nabla_1$.

Since $C_1M_1$ is seen from $B_1$ and $K_1$ at right angles, $B_1$, $C_1$, $K_1$, and $M_1$ are concyclic. Further, $B_1L_1$ is seen from $A_1$ and $M_1$ at right angles. Thus, the circumcircle of $B_1$, $C_1$, $K_1$, and $M_1$ equals that of $A_1$, $B_1$, $L_1$, and $M_1$.

Two similar triangles can only share the circumcircle if they are congruent (which can be confirmed with help of the Law of sines).

Finally, we have to show that the circumcenter of the six points $A_1$, $B_1$, $C_1$, $K_1$, $L_1$, $M_1$ is the symmedian point $X_6$ of $\Delta_0$. We compute the actual distances of the midpoint $M$ of the segment $A_1K_1$ to $\Delta_0$'s side lines and find

$$\begin{aligned}\overline{M\,[A_0,B_0]} &= 2cF\sigma^{-1},\\ \overline{M\,[B_0,C_0]} &= 2aF\sigma^{-1},\\ \overline{M\,[C_0,A_0]} &= 2bF\sigma^{-1},\end{aligned}$$

and thus, the homogeneous trilinear coordinates are

$$M = (a : b : c)$$

which confirms that $M$ equals the symmedian point $X_6$ of $\Delta_0$. □

From Lem. 1, we can deduce a simple linear construction of $\Delta_1$ (and $\nabla_1$) which is shown in Fig. 5: An arbitrary triangle $\Delta = A'B'C'$ with

$$A' \in [A_0, B_0],\ B' \in [B_0, C_0],$$
$$[A', B'] \perp [A_0, B_0]$$

similar to $\Delta_0$ is drawn, *i.e.*,

$$\sphericalangle C'A'B' = \sphericalangle C_0A_0B_0,$$
$$\sphericalangle A'B'C' = \sphericalangle A_0B_0C_0.$$

[1] Here, and in the following $X_i$ means the $i$-th point in Kimberlings's encyclopedia of triangle centers [4, 5].

The central similarity with center $B_0$ sends $C'$ to $C_1 \in [C_0, A_0]$, and thus, it maps $\Delta' \to \Delta_1$.

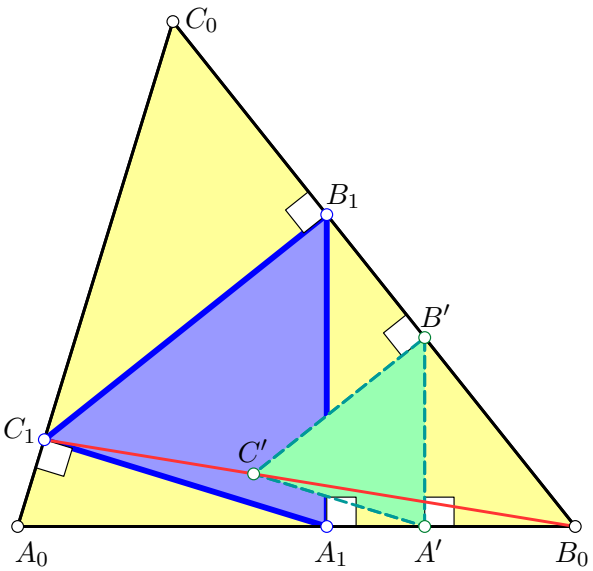


Figure 5: The construction of $\Delta_1$ is linear and uses the central similarity from $B_0$.

From this construction it is clear that there is a second triangle $\nabla_1 = K_1L_1M_1$ similar to $\Delta_0$ and inscribed into $\Delta_0$, but different from $\Delta_1$: We start with a triangle $\nabla = K'L'M'$ and let

$$L' \in [A_0, B_0], K' \in [C_0, A_0],$$
$$[K', L'] \perp [A_0, B_0]$$

with

$$\sphericalangle K'L'M' = \sphericalangle A_0B_0C_0,$$
$$\sphericalangle M'K'L' = \sphericalangle C_0A_0B_0.$$

Now, the similarity with center $A_0$ sends $K'L'M'$ to $K_1L_1M_1$.

## 2.2 Non-Euclidean planes

The case of the pseudo-Euclidean plane was the subject of Rem. 1 since its only difference is the hyperbolic projectivity on the ideal line (in the plane's projective extension).

In hyperbolic and elliptic geometry, there is still a projective mapping $\pi : [A_0, B_0] \to [A_0, B_0]$. However, since there is no ideal line, but rather an ideal conic, we miss a self-assigned ideal point on $[A_0, B_0]$. Thus, $\pi$ has up to two real fixed points:

**Theorem 2.** *In each generic triangle in the hyperbolic or elliptic plane, there exist two closed semi-orthogonal paths for a particular chosen ordering of side lines.*

The reality of the fixed points mentioned in Thm. 2 is clear in the hyperbolic and in the elliptic case: Let $\omega$ denote the absolute conic. Each pair $(V_i, V_j)$ of proper vertices of the triangle and the pair of absolute points $(A_1, A_2) = [V_i, V_j] \cap \omega$ of $[V_i, V_j]$ are not entangled. Therefore, there are two real fixed points on $[V_i, V_j]$, see [2, p. 254].

Fig. 6 shows a triangle $\Delta_0 = A_0B_0C_0$ in the projective model of the elliptic plane together with the two closed semi-orthogonal paths to a chosen ordering of $\Delta_0$'s side lines.

There are two different closed semi-orthogonal paths in a triangle in the elliptic or in the hyperbolic plane. Since the projective mapping $\pi : [A_0, B_0] \to [A_0, B_0]$ is hyperbolic in elliptic as well as hyperbolic geometry, there are four closed semi-orthogonal (triangular) paths in a generic

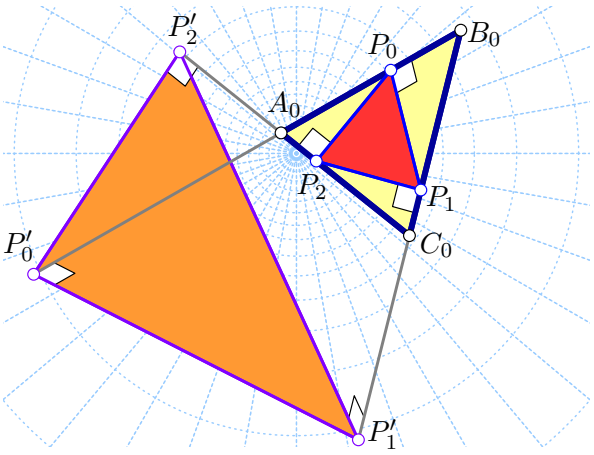


Figure 6: Two closed semi-orthogonal paths in a triangle $\Delta_0 = A_0B_0C_0$ of the elliptic plane. The paths are starting with $[P_0, P_1]\perp_e[A_0, B_0]$ and $[P_0', P_1']\perp_e[A_0, B_0]$, respectively.

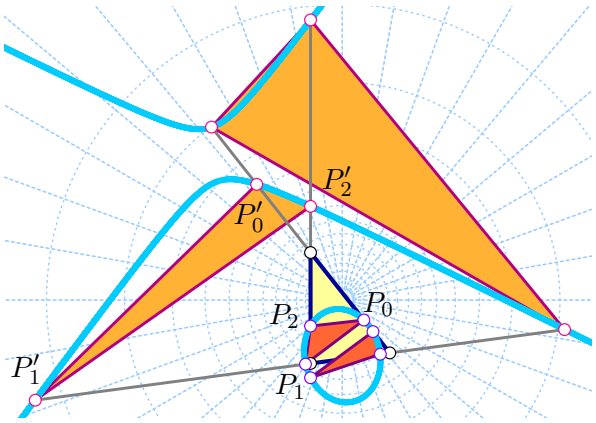


Figure 7: There are four closed semi-orthogonal paths in a triangle in the elliptic plane. Two by three vertices gather on a conic: three points from an $[A_0, B_0] - [B_0, C_0] - [C_0, A_0]$ path and three vertices from an $[A_0, B_0] - [C_0, A_0] - [B_0, C_0]$ path.

triangle. Fig. 7 shows these four closed semi-orthogonal paths in a triangle in the elliptic plane. This four-fold symmetry resembles the four-fold symmetry in Universal Hyperbolic Geometry (cf. [8, 9]) and shows up when classical triangle geometry is also studied from the viewpoint of projective geometry, see [7].

Neither in the elliptic nor in the hyperbolic plane we can use Thales's theorem in order to show that two of the triangular paths share a circumconic as illustrated in Fig. 7.

# 3 Infinite sequences of inscribed triangles

In this section, we return to Euclidean geometry in order to attack the main problem.

We have seen that $\Delta_0$ and $\Delta_1$ are similar triangles. Consequently, the triangle $\Delta_2$ inscribed into $\Delta_1$ whose vertices $A_2$, $B_2$, $C_2$ are obtained in the same way as $A_1$, $B_1$, $C_1$ is also similar to $\Delta_1$, and thus, to $\Delta_0$. This procedure can be repeated arbitrarily often which yields a sequence of similar triangles $\Delta_0$, $\Delta_1$, $\Delta_2$, $\Delta_3$, $\Delta_4$, ... for a particular triangle $\Delta_0$.

Due to the construction of $\Delta_1$, subsequent edges $A_iA_{i+1}$ and $A_{i+1}A_{i+2}$ of the polygon $A_0A_1A_2A_3A_4\ldots$ are orthogonal. Further, the edges $A_iA_{i+1}$ and $A_{i+2}A_{i+3}$ are antiparallel. The same holds true for the polygons $B_0B_1B_2\ldots$ and $C_0C_1C_2\ldots$. Fig. 8 shows the polygon $A_0A_1A_2A_3\ldots$, while Fig. 9 shows the six discrete logarithmic spirals encircling two different limits.

Now, we want to show that the triangles $\Delta_i$ and $\nabla_i$ converge to a point as $i \to \infty$. In this case, it is not necessary to apply shape functions like in [3]. We need some other

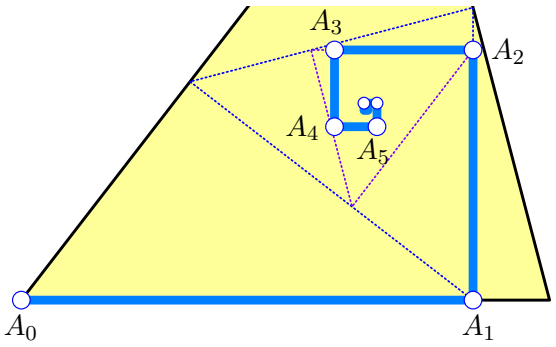


Figure 8: The discrete logarithmic spiral formed by $A_0$, $A_1$, ... winding towards a limit.

prerequisites. With (7) it is easy to verify that the side lengths $a_1 = \overline{B_1C_1}$, $b_1 = \overline{C_1A_1}$, $c_1 = \overline{A_1B_1}$ of $\Delta_1$ are

$$a_1 = a\lambda, \quad b_1 = b\lambda, \quad c_1 = c\lambda$$

where $\lambda$ is the scaling factor of the similarity $\Delta_0 \to \Delta_1$ which can be computed from $a$, $b$, and $c$ via

$$\lambda = 4F\sigma^{-1} \tag{8}$$

where $F$ equals the area of $\Delta_0$. This allows us to express the radius of the circle $l$ (cf. Thm. 1) in terms of $\Delta_0$'s side lengths:

**Corollary 1.** *The radius of $l$ equals*

$$R_1 = \frac{abc}{a^2 + b^2 + c^2}.$$

*Proof.* Lengths are scaled with the factor $\lambda$ when applying the similarity $\Delta_0 \to \Delta_1$. Thus, the circumradius $R_0$ changes to $R_1 = R_0\lambda$ with $\lambda$ given in (8). According to the Law of sines, $R_0 = \frac{abc}{4F}$, and thus, $R_1 = abc\sigma^{-1}$. □

The fact that the sequence of triangles $\Delta_0$, $\Delta_1$, $\Delta_2$, ... (as well as the sequence of all $\nabla_i$) consists of scaled versions of the initial triangle $\Delta_0$ together with the fact that the scaling factor depends on the side lengths of each triangle in the same way (cf. Eq. (8)) makes the traces of $\Delta_0$'s vertices a special polygon. For example, the segment $A_1A_2$ is orthogonal to $A_0A_1$ and $\overline{A_1A_2} = \lambda \cdot \overline{A_0A_1}$. This holds true for any pair $(A_iA_{i+1}, A_{i+1}A_{i+2})$ of subsequent segments. Thereby, a sequence of discrete equiform motions (consisting of a quarter turn and a constant scaling) *moves* the polygon $A_0A_1A_2\ldots$ into itself and we can say that $A_0A_1A_2\ldots$ is invariant under the sequence of discrete equiform motions. In

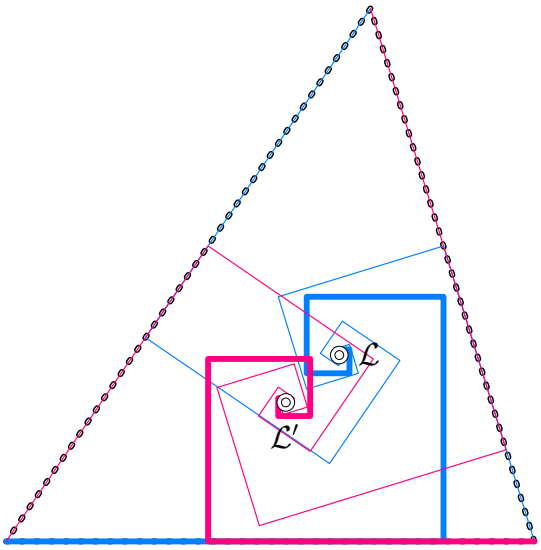


Figure 9: The six discrete logarithmic spirals orbiting the limit points $\mathcal{L}$ and $\mathcal{L}'$.

the smoth case, the trace of a point undergoing one-parameter equiform motion with constant parameter is a logarithmic spiral. Therefore, we can call $A_0A_1A_2\ldots$ a *discrete logarithmic spiral*. Fig. 9 shows the six discrete logarithmic spirals traced by

the three vertices of $\Delta_0$ undergoing the two independent sequences of discrete equiform motions.

Now, we are able to state and prove:

**Theorem 3.** *The limit position $\mathcal{L}$ of all points $A_i$, $B_i$, or $C_i$ is the first Brocard point of $\Delta_0$ with homogeneous trilinear coordinates*

$$\mathcal{L} = (ac^2 : ba^2 : cb^2) \tag{9}$$

*while the limit $\mathcal{L}'$ of all points $K_i$, $L_i$, or $M_i$ is the second Brocard point of $\Delta_0$,* i.e., *in terms of homogeneous trilinear coordinates*

$$\mathcal{L}' = (ab^2 : bc^2 : ca^2). \tag{10}$$

*Proof.* With the initial choice of the coordinate frame, we can find the limit position

$$\mathcal{L} = \lim_{i\to\infty} A_i.$$

The $x$- and $y$-coordinate $x_{\mathcal{L}}$ and $y_{\mathcal{L}}$ are

$$\begin{aligned} x_{\mathcal{L}} &= \overline{A_0A_1} - \overline{A_2A_3} + \overline{A_4A_5} - \overline{A_6A_7} \pm \ldots, \\ y_{\mathcal{L}} &= \overline{A_1A_2} - \overline{A_3A_4} + \overline{A_5A_6} - \overline{A_7A_8} \pm \ldots. \end{aligned} \tag{11}$$

The similarity $\Delta_i \to \Delta_{i+1}$ changes lengths by scaling them with the factor $\lambda$, *i.e.*,

$$\overline{A_iA_{i+1}} = \lambda^k \cdot \overline{A_{i+k}A_{i+k+1}}$$

for $i, k \in \{0, \ldots, n\}$. Consequently, the coordinates $x_{\mathcal{L}}$ and $y_{\mathcal{L}}$ from (11) change to

$$\begin{aligned} x_{\mathcal{L}} &= \overline{A_0A_1}\ (1 - \lambda^2 + \lambda^4 \mp \ldots), \\ y_{\mathcal{L}} &= \overline{A_0A_1}\lambda(1 - \lambda^2 + \lambda^4 \mp \ldots). \end{aligned} \tag{12}$$

The length of the segment $\overline{A_0A_1}$ follows from (1), (7) with (2) and is already given in (4):

$$\overline{A_0A_1} = t = 2b^2c\sigma^{-1}.$$

We let

$$\tau := a^2b^2 + b^2c^2 + c^2a^2 \tag{13}$$

and with (8), we can infer

$$\lambda = \sqrt{\frac{2\tau - a^4 - b^4 - c^4}{2\tau + a^4 + b^4 + c^4}} < 1$$

for any admissible choice of $a$, $b$, and $c$. Consequently, the infinite alternating sum of even powers of $\lambda$ attains the value

$$\frac{1}{1+\lambda^2}$$

which gives

$$\mathcal{L} = \frac{b^2c}{2\tau}(\sigma, 4F). \tag{14}$$

Note that $\mathcal{L}$ given in (14) is at the same time the limit of $B_i$ and $C_i$ too.

The $y$-coordinate of $\mathcal{L}$ in (14) equals the distance of $\mathcal{L}$ to the line $[A_0, B_0]$. Therefore, it is the third actual trilinear coordinate of $\mathcal{L}$. It is elementary to compute the first and second actual trilinear coordinate of $\mathcal{L}$ and it turns out that they can be obtained by cyclically replacing $a$, $b$, $c$ once and twice in $2b^2cF\tau^{-1}$. We observe that both $F$ and $\tau$ are cyclic symmetric in $a$, $b$, $c$, and therefore, they do not change. For the sake of simplicity, we aim at homogeneous trilinear coordinates of $\mathcal{L}$ which allows us to cancel cyclic symmetric factors as long as they are common to all coordinate functions. So, we obtain (9).

A comparison of (9) with the trilinear representation of the first Brocard point given in [6] confirms that $\mathcal{L}$ is indeed the first Brocard point.

The calculations do not really differ if we compute the limit position $\lim_{i\to\infty} K_i = \mathcal{L}'$. In this case, it is beneficial to start at $B_0 = (c, 0)$ and determine

$$\mathcal{L}' = \begin{pmatrix} c \\ 0 \end{pmatrix} + \\ + \overline{B_0L_1} \begin{pmatrix} -1 + \lambda^2 - \lambda^4 \pm \dots \\ \lambda(1 - \lambda^2 + \lambda^4 \mp \dots) \end{pmatrix}$$

where $\overline{B_0L_1} = 2a^2c\sigma^{-1}$ which results in

$$\mathcal{L}' = \frac{c}{2\tau}\left(b^2c^2 - a^4 + \tau, 4a^2F\right). \qquad (15)$$

In the same way as above, we end with

$$\mathcal{L}' = (ab^2 : bc^2 : a^2c). \qquad \square$$

**Remark 2.** *The two limit positions $\mathcal{L}$ and $\mathcal{L}'$ are no triangle centers: Of course, the trilinear representation is apparently cyclic symmetric in the side lengths $a$, $b$, $c$ of $\Delta_0$, but, they do not satisfy the norming condition: If $f(a, b, c)$ is a center function, then it also has to satisfy $|f(a, b, c)| = |f(a, c, b)|$ in order to make $(f(a, b, c) : f(b, c, a) : f(c, a, b))$ a center.*

Now, we show

**Theorem 4.** *The point $\mathcal{L}$ is the only (real and proper) common point of the three Thaloids of the segments $A_0A_1$, $B_0B_1$, $C_0C_1$.*

*The point $\mathcal{L}'$ is the only (real and proper) common point of the three Thaloids of the segments $A_0K_1$, $B_0L_1$, $C_0M_1$.*

*Proof.* From the asymptotic point $\mathcal{L}$ of the discrete logarithmic spiral $A_0A_1A_2\dots$, any segment $A_iA_{i+1}$ can be seen at a right angle, since each subsequent segment of the discrete logarithmic spiral corresponds to a quarter turn plus a scaling with the factor $\lambda$. This is also the case for the segments $B_iB_{i+1}$ and $C_iC_{i+1}$.

For the same reasons, the limit $\mathcal{L}'$ of the second sequence is simultaneously located on three Thaloids. $\square$

Thm. 4 provides a very elegant and elementary construction of the two Brocard points $\mathcal{L}$ and $\mathcal{L}'$. This construction seems not to be mentioned in the literature.

Fig. 10 shows the three Thaloids through $\mathcal{L}$. Clearly, there are also three Thaloids

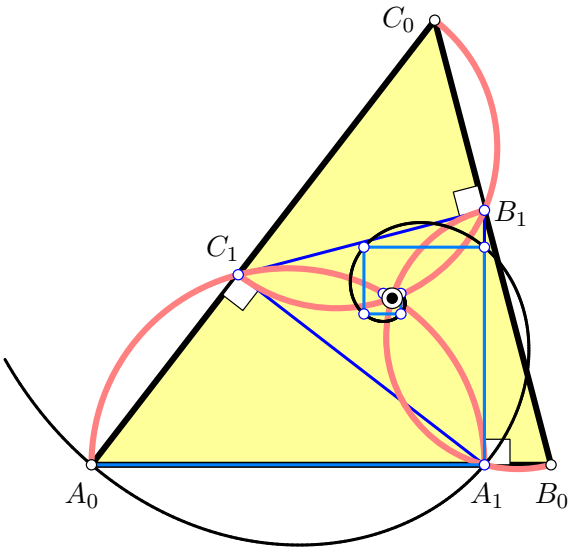


Figure 10: Three Thaloids concur in $\mathcal{L}$.

passing through $\mathcal{L}'$.

As a consequence of Thm. 3, the two limits of the triangle tunnels are located on a special self-isotomic pivotal cubic K012 (cf.

[1]), better known as the Tucker-Brocard cubic $\mathcal{T}$. Only a few centers from Kimberling's list [5] are known to lie on $\mathcal{T}$: the symmedian point (also Lemoine point or Grebe point) $X_6$, its isotomic conjugate $X_{76}$ (the third Brocard point), and further the two centers $X_{880}$ and $X_{882}$. ($X_{882}$ lies on the Brocard axis $[\mathcal{L}, \mathcal{L}']$.) Fig. 11 shows the tunnel limits (Brocard points) together with the Tucker-Brocard cubic $\mathcal{T}$ and the centers $X_6$, $X_{76}$, $X_{880}$, $X_{882}$.

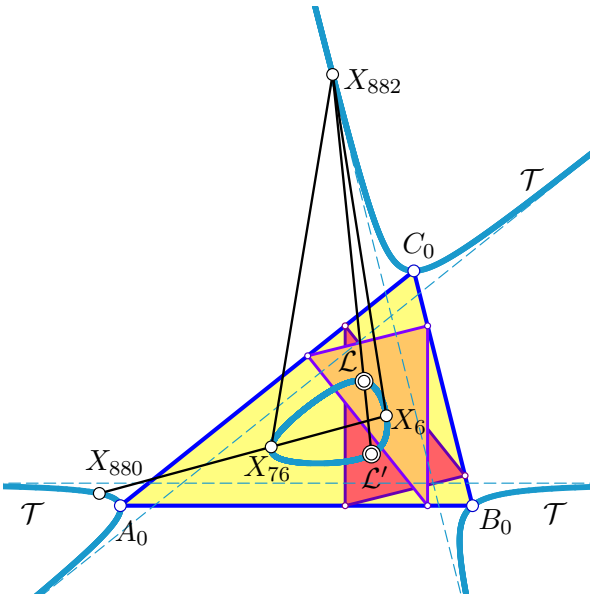


Figure 11: The Tucker-Brocard cubic contains the first and second Brocard point $\mathcal{L}$ and $\mathcal{L}'$. besides $X_6$, $X_{76}$, $X_{880}$, and $X_{882}$.

# 4 Conclusion and open problems

The semi-orthogonal paths in quadrilaterals will, in general, not be similar to the initial quadrilateral, for there exists no equiform transformation that maps two quadrilaterals onto each other even when they agree in their interior angles. Nevertheless, the iteration of the computation of semi-orthogonal paths in a quadrilateral produces sequences of shrinking and nested quadrilaterals which preserve their interior angles. Fig. 12 shows an example. In fact, there exist up to six such sequences in a generic quadrilateral. Apparently, there exists an attractor for the six different semi-orthogonal paths in a quadrilateral. It would be interesting to find a tool to compute the limits, if they exist. Shape functions for quadrilaterals as used for triangles in [3] or for generic $n$-gons defined in [10] could help.

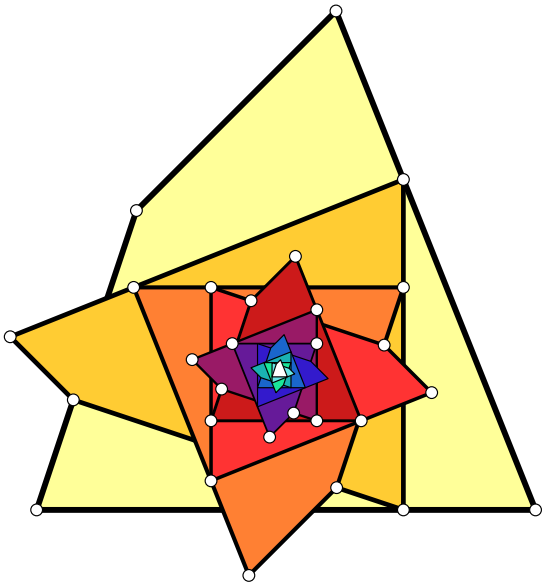

Figure 12: A sequence of shrinking and nested closed semi-orthogonal paths in a quadrilateral. It is obvious that interior angles remain unchanged.

Only the case of cyclic quadrilaterals seems hopeful. Since the measures of interior

angles are preserved during the transition from one quadrilateral to the next in the sequence of semi-orthogonal paths, so is there sum or difference. In a cyclic quadrilateral opposite interior angels sum up to $\pi$, *i.e.*, $\sphericalangle ABC + \sphericalangle CDA = \pi$ and $\sphericalangle BCD + \sphericalangle DAB = \pi$ and so do the sums of the opposite (interior) angles in their semi-orthogonal paths, see Fig. 13. Hence, the semi-orthogonal path of a cyclic

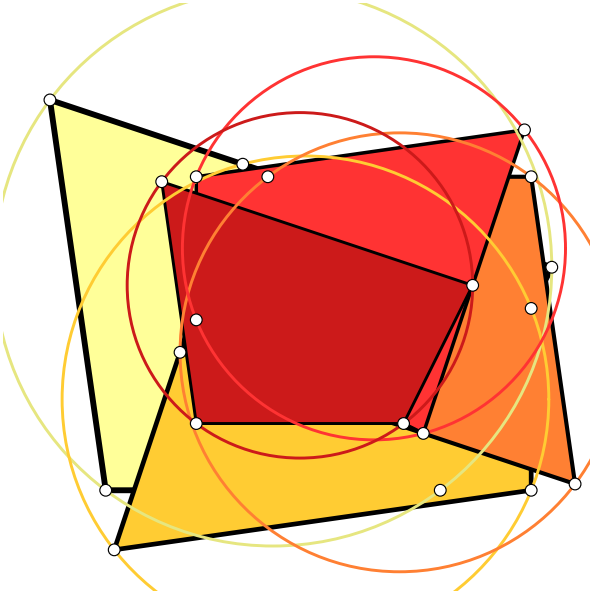

Figure 13: The first four semi-orthogonal paths of a cyclic quadrilateral are similar and perspective to the initial quadrilateral.

quadrilateral is again a cyclic quadrilateral. Numerical experiments show that each $4i$-th semi-orthogonal path of a cyclic quadrilateral is similar and perspective to the initial cyclic quadrilateral ($i \in \mathbb{N}$). The perspector is common to all pairs of quads, cf. Fig. 14.

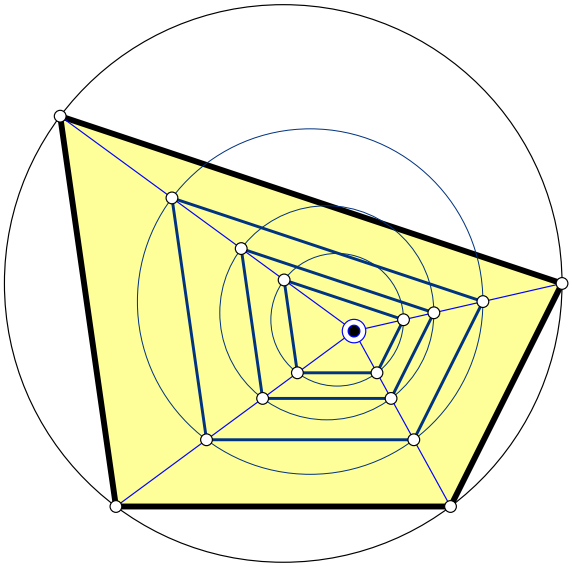

Figure 14: The $4^{\text{th}}$, $8^{\text{th}}$, and $12^{\text{th}}$ semi-orthogonal path of a cyclic quadrilateral are similar and perspective to the initial quadrilateral. The perspector could be see as the limit of the sequence of semi-orthogonal paths.

# References


[1] B. Gibert: *Tucker-Brocard cubic.* Available at: `http://bernard.gibert.pagesperso-orange.fr/Exemples/k012.html`

[2] G. Glaeser, H. Stachel, B. Odehnal: *The Universe of Concis.* From the ancient Greeks to $21^{\text{st}}$ century developments. Springer-Spektrum, Springer-Verlag, Heidelberg, 2016.

[3] M. Hajja: *On nested sequences of triangles.* Result. Math. **54**/3 (2009), 289–299.

[4] C. Kimberling: *Triangle Centers and Central Triangles.* (Congressus Numerantium Vol. 129) Utilitas Mathematica Publishing, Winnipeg, 1998.

[5] C. Kimberling: *Encyclopedia of Triangle Centers.* Available at: `http://faculty.evansville.edu/ck6/encyclopedia`

[6] C. Kimberling: *Bicentric Pairs of Points and Related Triangle Centers.* Forum Geometricorum **3** (2003), 35–47.

[7] B. Odehnal: *Generalized Gergonne and Nagel Points.* Beitr. Alg. Geom. **51**/2 (2010), 477–491.

[8] N. Le, N.J. Wildberger: *Universal Affine Triangle Geometry and Four-fold Incenter Symmetry.* KoG **16** (2012), 63–80.

[9] N. Le: *Four-Fold Symmetry in Universal Triangle Geometry.* PhD thesis, University of New South Wales, Australia, 2015.

[10] E.L. Wachspress: *A rational basis for function approximation.* Lecture Notes in Mathematics. Vol. 228, Springer, New York, 1971.